Accepted Manuscript

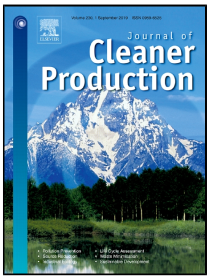

Multi-attribute decision-making approach for *Aegle marmelos* pyrolysis process using TOPSIS and Grey Relational Analysis: Assessment of engine emissions through novel Infrared thermography

P. Baranitharan, K. Ramesh, R. Sakthivel

PII: S0959-6526(19)32150-X

DOI: 10.1016/j.jclepro.2019.06.188

Reference: JCLP 17357

To appear in: *Journal of Cleaner Production*

Received Date: 02 August 2018

Accepted Date: 17 June 2019

Graphical Abstract

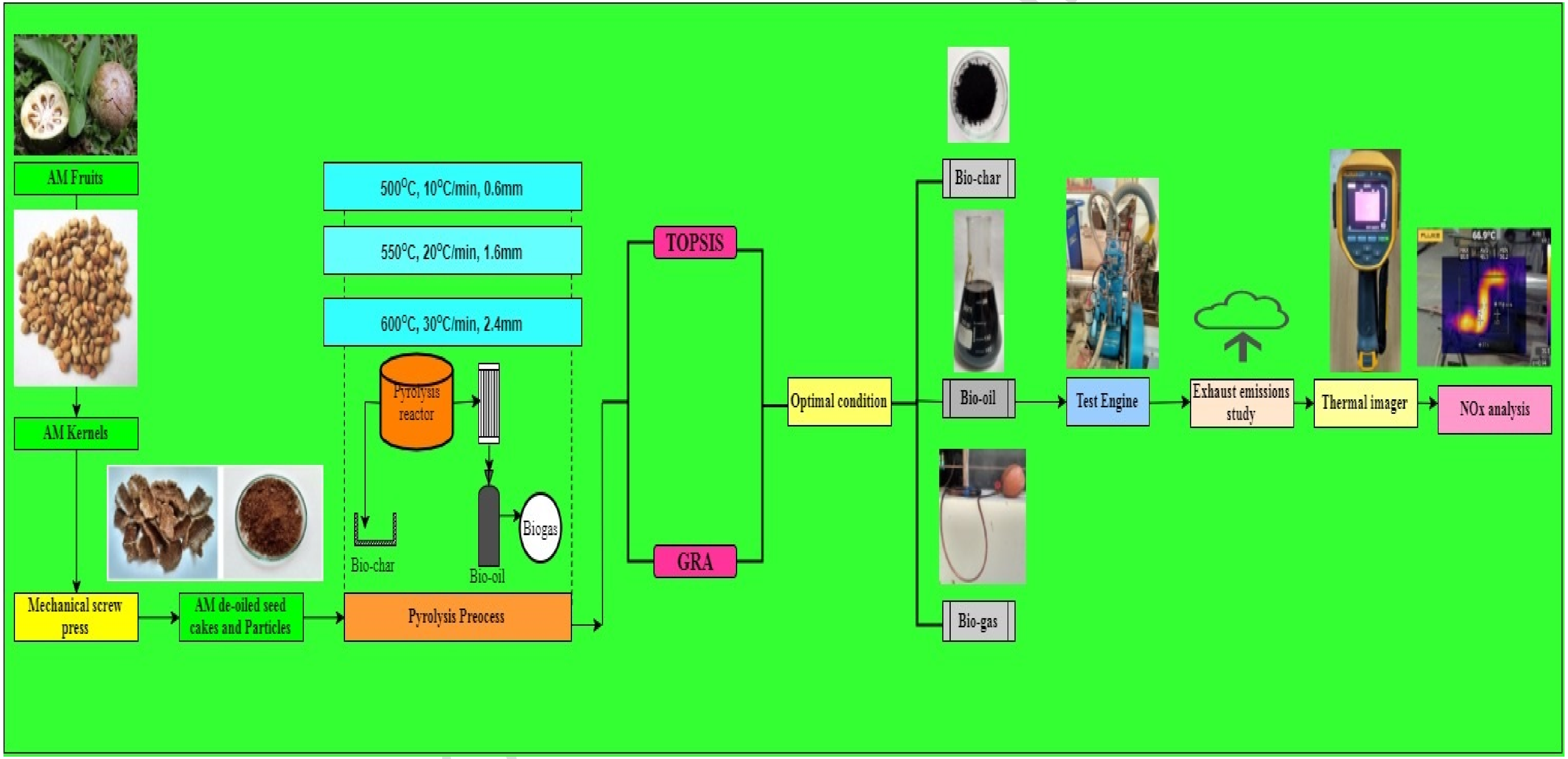

Multi-attribute decision-making approach for *Aegle marmelos* pyrolysis process using TOPSIS and Grey Relational Analysis: Assessment of engine emissions through novel Infrared thermography

P.Baranitharan*[1], K.Ramesh[1], R.Sakthivel[2]

[1]Department of Mechanical Engineering, Government College of Technology, Coimbatore, India-641013

[2]Department of Mechanical Engineering, Amrita School of Engineering, Coimbatore, Amrita Vishwa Vidyapeetham, India

E-mail:baraniparamasivam@gmail.com*[1],kramesh@gct.ac.in[2],sakthivelmts@gmail.com[3]

*Corresponding author: Tel: +91 8973506306, e-mail: baraniparamasivam@gmail.com, Postal address: 2/306 H, Shaj Bhaj Nagar, Blue Hills Avenue, Bellathi post. Karamadai SO. Mettupalayam Taluk.641104. Coimbatore Dist. Tamil Nadu. India.

Abstract

This research focuses on the selection of the optimum process parameters for *Aegel marmelos* (AM) pyrolysis experiment based on multi-objective decision-making techniques. This investigation presents the optimization report for obtaining maximum pyrolysis oil from AM de-oiled seed cake through thermochemical conversion (pyrolysis) process. The pyrolysis process has been conducted according to L_{27} orthogonal array with chosen input control factors such as pyrolysis temperature (°C), heating rate (°C/min) and biomass particle size (mm). The output response parameters measured are the bio-oil yield, bio-char yield and biogas yield. The multi-objective decision-making approach namely Technique for order preference by similarity to ideal solution (TOPSIS) and Grey relational analysis (GRA) techniques are employed to determine the optimum pyrolysis process parameters to maximize the yield of AM bio-oil. The optimized values of pyrolysis temperature (PT), heating rate (HR) and feedstock particle size (PS) are 600°C, 10°C/min and 0.6 mm. At peak engine loading condition, 20% AM bio-oil + 80% diesel fuel blend (AM20) emit lower carbon dioxide (CO_2=8.68%) and oxides of nitrogen (NOx=1401 ppm) emissions as compared with diesel (D) CO_2 (10.33%) and NOx (1511 ppm) emissions. The association between exhaust gas temperature and NOx emission was inferred using a novel approach of thermal imager by sensing the infrared rays from the hot surface of the exhaust port. Infrared thermal images are

captured during the engine operations fuelled with bio-oil at the optimum pyrolysis conditions concluded by TOPSIS and GRA results (PT=600°C, HR=10°C/min and PS=0.6 mm). According to the thermal imaging result, AM20 blend produces the lower amount of NOx emissions compared with neat diesel and it is suggested that AM bio-oil can be used as engine fuel instead in order to preserve the eco-system stability and biodiversity.

Keywords: *Aegle marmelos*; Pyrolysis; TOPSIS; GRA; NOx emission; Thermal Imager.

Nomenclature

AM	*Aegle marmelos*
AM 20	20% *Aegle marmelos* bio-oil + 80% diesel
ASTM	American Society for Testing and Materials
bTDC	Before the top dead centre
CC	Closeness coefficient
CI	Compression ignition
CO	Carbon monoxide (%)
CO_2	Carbon dioxide (%)
CR	Compression ratio
D	Neat diesel
Dp	Biomass particle diameter (mm)
D $(Tij)_{(x*y)}$	TOPSIS design matrix
GRA	Grey relational analysis
GRC	Grey relational coefficient
GRG	Grey relational grade
HC	Hydrocarbons (ppm)
HR	Heating rate (ºC)
i	Trial number
IR	Infrared
J_1	Set of beneficial attribute
J_2	Set of non-beneficial attribute
k	Comparability sequence
MCC	Mean closeness coefficient
MGRG	Mean grey relational grade
$\max g_i(k)$	Maximum value of $g_i(k)$ for kth response
$\min g_i(k)$	Minimum value of $g_i(k)$for kth response
NOx	Oxides of nitrogen (ppm)
nij	The normalized value of the design matrix
PCA	Principal component analysis
PS	Biomass particle size (mm)
PT	Pyrolysis temperature (ºC)
RCC	Relative closeness coefficient
RSM	Response surface methodology
S_i^+	Positive separation measures
S_i^-	Negative separation measures
T	Temperature
TGA	Thermogravimetric analysis

TOPSIS	The technique for order preference by similarity to an ideal solution
Tij	The measure of the j[th] attribute to the i[th] alternative
x	Alternatives/Test trials
$x_i(k)$	The normalised value of output
y	Attributes/Output response
ξ_{ij}	Weighted normalized matrix
ξ^{+}	Positive ideal solution
ξ^{-}	Negative ideal solution
$\Delta_{oi}(k)$	Deviation sequence
Δ_{min}	Minimum deviation sequence
Δ_{max}	Maximum deviation sequence
φ	Distinctive coefficient
$\varphi_i(k)$	Grey relational coefficient
ϑ_i	Grey relational grade

1. Introduction

Fossil fuels play a vital role in the transportation sector but emit harmful gases like carbon mono oxide, oxides of nitrogen, hydrocarbons and sulphur content gases etc. which in turn augments the global temperature. The Shortage of fossil fuel resources and its related environmental problems grasped great attention towards bio-fuel research (Bordoloi et al., 2016). Biofuel usage decreases the global warming rate by adopting the closed carbon cycle thereby reducing greenhouse emissions (D'Alessandro et al., 2016; Mi et al., 2016). Foremost benefits of biofuels are eco-friendliness, renewability and bio-degradability (Knothe et al., 2006). Biochemical and thermochemical conversion technologies are commonly used to convert the biomass into solid (bio-char), liquid (bio-oil) and gas (biogas) products. As compared to biochemical routes, thermochemical conversion possesses more advantages in terms of time consumption and decomposing C_5 sugars (Bordoloi et al., 2016). Pyrolysis is one of the most capable techniques among the available biomass conversion methods (Halim and Swithenbank, 2016). In the pyrolysis process, biomass is heated in the absence of oxygen atmosphere to derive useful products like bio-oil, biochar and biogas (Abas et al., 2018). The notable advantages of pyrolysis products are that they are eco-friendly, reusable and valorised into fuels and chemicals (Halim and Swithenbank, 2016).

From wide literature reviews, it can be inferred that significant works have been done in AM cold pressed oil. Very few researchers carry out their research in the study of AM vegetable oil properties and diesel engine performance and emission characteristics fuelled with AM seed oil blends (Katagi et al., 2011). AM tree falls under the Rutaceae family (Paramasivam et al., 2018) and it is generally seen in south Indian Shiva temples

(Baranitharan et al., 2019). AM seedswere collected from its matured fruits. The thermal properties of AM seed cake were characterized with the help of thermo gravimetric analysis.

Anupam et al. (2016) optimized the process parameters of *Leucaenal eucocephala* bark using RSM (Response surface methodology) method and determined the optimal pyrolysis temperature and time (Anupam et al., 2016). Optimization of the lignin pyrolysis of wood was done using the PCA (Principal component analysis) method (shen How and Lam, 2018). Mohammed et al. (2016) optimized the napier grass pyrolysis oil using RSM in terms of pyrolysis temperature, heating rate and nitrogen gas flow rate (Mohammed et al., 2017b). Mohammed et al. (2017a) optimized the pyrolysis temperature, heating rate and nitrogen flow rate of Bambara groundnut using RSM tool and obtained the optimized parameters of 600ºC, 50ºC/min and 11 L/min respectively. The author also employed L_{27} orthogonal array to design the experiments and analysed the effect of each parameter on bio-oil yield through Taguchi method. Considering the pyrolysis process, the quality of experiments was based on the yield of bio-oil. So, any numbers of quality characteristics can be considered for the selection of best pyrolysis parameters (Mohammed et al., 2017a). Taguchi methodology is restricted to optimizing single objective problems (Sahu et al., 2016). In the present research scenario, it is inevitable to solve multi-criteria problems in complex engineering systems. In this view, numerous techniques are offered like Technique for order preference by similarity to ideal solution (TOPSIS) and Grey relational analysis (GRA). GRA tool works under the grey system theory and suitable for solving multi-objective problems with the complex relationship between several factors and variables (Kuo et al., 2008). The GRA technique tool decreases the difficulty and increases the overall efficiency of the problems (Liu and Cheng, 2016). TOPSIS method is simple and efficient (Guo and Zhao, 2015) with a multi-objective decision-making technique used to solve the multiple systems (Hussein et al., 2016).

Generally, bio-oil is rich in oxygenated compounds due to which it can be directly used as an engine fuel along with baseline diesel fuel without any engine modifications (Baranitharan et al., 2018; Sakthivel et al., 2018). Using fossil fuels as a fuel in internal combustion engine operation emits harmful gases (Halim and Swithenbank, 2016). As compared to baseline diesel emission, pyrolysis bio-oil emits less pollutant (López et al., 2008). Compression ignition (CI) engine emit a higher amount of NOx emission value to the atmosphere. The thermal imaging method is exhibited to be a novel technique for heat distribution measurement investigations (Merino-Pérez et al., 2015). The equilibrium concentration is of nitric oxidesis very high at high combustion chamber temperatures, which is also encounted near the stoichiometric combustion. Zeldovich mechanism is a simple reaction mechanism which defines the formation of thermal NOx which is given as Eqns. (1) and (2),

$$N_2 + O \leftrightarrows N + NO \quad (1)$$

$$N + O_2 \rightleftarrows O + NO \quad (2)$$

Hence, by evaluating the zeldovich mechanism, it is obvious that NOx emission value greatly depends on the combustion chamber temperature. Hence, among the exhaust emission, NOx can be investigated through green technology aided thermal images with better understanding. Shameer and Ramesh (2017a,b) studied the relationship between NO_X emission level and in-cylinder temperature via FLUKE thermal imager and concluded that combustion temperature is a key parameter to the oxides of nitrogen emission measurement (Shameer and Ramesh, 2017a, b). The Author used thermography to measure the radiation emitted by an object at different points from a hot source in the infrared spectrum and converted it into source temperature (Garcia-Gonzalez et al., 2016; Ramesh et al., 2019). The novel approach of using FLUKE-Thermal imager for analysing the relationship between exhaust gas temperature and engine test NOx emission characteristics has been executed in this research. Table 1 presents a comparison of previous biofuel studies using TOPSIS and GRA optimization techniques.

Table 1 Comparison of previous bio-fuel studies using TOPSIS and GRA techniques

Tools	Investigation	Parameters	Materials	Conclusion	Reference
TOPSIS	Optimization of feed stock material to obtain a maximum bio-oil yield	Lignin cellulose, Hemicellulose, Volatile matter, Fixed carbon, Moisture content, Ash content	Rice straw, Sunflower shell, Hardwood, Wheat straw, Palm shell	High volatile matter content (79.2 wt%) Hardwood biomass selected as the bestfeedstock material for pyrolysis.	(Madhu et al., 2018)
TOPSIS	Optimization of CI engine	Charge inlet temperature,	65% Diesel + 25% Bael-oil + 10%	Charge inlet temperature=320K,	(Muniappan and

	parameters to obtain better performance and emission characteristics	Exhaust gas recirculation	Diethyl ether blend	Exhaust gas recirculation=30% gives better engine characteristics.	Rajalingam, 2018)
GRA	Optimize the influence factor of sea wood particle combustion	Bed temperature, Fluidization velocity, Materials height	Sea wood particles	Bed temperature has a great influence on the bed combustion	(Wang et al., 2013)
GRA	Optimization of bio-gas production process parameters	Solid concentration, Temperature of food waste, Co-digestion of poultry waste	Anaerobic digested food waste	Solid concentration=7.5%, Temperature of food waste= 50ºC, Co-digestion of poultry waste= 30%, selected as an optimal condition	(Senthilkumar et al., 2016)
GRA	Performance optimization of CI engine fuelled with Chicken-waste bio-diesel	Blend, Compression ratio (CR), Injection timing, Injection pressure	Chicken-waste bio-diesel	Blend 10 fuel, CR18, Injection pressure 220 bar, 19º bTDC (Before top dead centre) engine parameters combination were delivered better engine performance.	(Hussain et al., 2014)

Numerous literature studies reveal that huge research works have been focused on optimizing single objective problem in the pyrolysis process. Very few works were carried out in the multi-objective optimization of pyrolysis experiments. To the best of author's knowledge, no significant works have been carried out in the utilization of TOPSIS and GRA tools for optimizing the AM pyrolysis process. In order to fill this gap, the present research focuses to apply TOPSIS technique for optimizing the process parameters of the AM pyrolysis process. The primary objective of this work is to examine the effect of each process parameters like pyrolysis temperature, heating rate and particle size on product yield. The next step mainly focuses to convert all process parameters into a single objective with the help of TOPSIS and GRA techniques.

2. Materials and Methods

2.1 *Aegel marmelos* biomass and pyrolytic oil

The fresh AM seed kernels were crushed by using a mechanical screw press to extract raw oil. During the extraction process, the remaining non-edible waste seed cake was collected and used as the feedstock for pyrolysis in this present research work.

Fig.1a AM seed cake

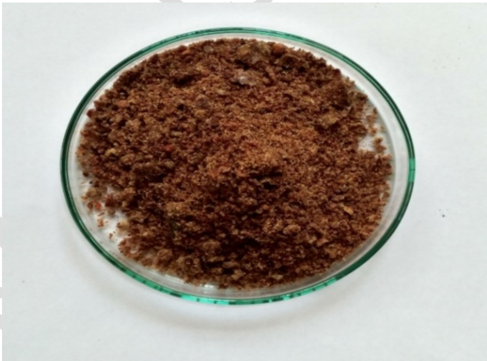

Fig.1b AM seed cake sieved particles

Figures 1a and 1b shows AM de-oiled seed cake and sieved powdered particles. The moisture content of collected AM de-oiled seed cake was removed through drying in sunlight. The proximate and ultimate analyses of biomass werecarried out as per (American Society for Testing and Materials) ASTM D3172-07a and ASTM D5291-96 (Bordoloi et al., 2016). Physical and chemical properties of bio-oil such as calorific value (Bomb calorimeter), kinematic viscosity (Redwood viscometer), flash point and fire point (Pensky Martin closed cup apparatus), cetane number (Ignition quality tester),acid number (Potentiometric titration) and density (Density meter) of bio-oil were determined as per ASTM standards.

2.2 Taguchi experimental design approach

Geneichi Taguchi developed a tool for designing the best quality system (Chen et al., 2014). In this method, the experimental design and quality loss function are related by Taguchi tool to suggest an effective design of experiment method through a systematic approach for optimizing the system parameters with fewer trials. In this present research, three input factors (3) with three levels (3) full factorial design has been implemented (3^3=3x3x3=27 trial). The L_{27} orthogonal array is used to study the entire process parameters combined with the lesser experimental trials and it is a cost-effective and time-saving technique for optimizing the process parameters. Minitab 17 is used in this study to perform optimal calculations by employing design L_{27} for 3 levels design and 3 control factors which afford 27 experimental trials.

In the present investigation, three pyrolysis parameters such as pyrolysis temperature (°C), heating rate (°C/min) and particle size (mm) were selected according to the literature review and expert advice. All the input control factors along with their corresponding levels are given in Table 2.

Table 2 Control factors and their levels

Input parameters	**Unit**	**Level 1**	**Level 2**	**Level 3**
Pyrolysis temperature (PT)	°C	500	550	600
Heating rate (HR)	°C/min	10	20	30
Feed stock particle size (PS)	mm	0.6	1.6	2.4

2.3 Technique for Order Preference by Similarity to Ideal Solution method

TOPSIS technique was presented by Hwang and Yoon (Anupam et al., 2014). TOPSIS technique is a multi-objective decision-making approach that assists to evaluate the better optimum results among the large size of the alternative solution. TOPSIS is established by the idea that the selected alternatives should have a minimum distance from the positive ideal consequences and maximum from the negative ideal outcomes for solving a multi-attribute decision-making problem. The positive ideal consequences are a collection of all greatest values, whereas the farthest ideal results are obtained by poorest values achievable of criteria. It is an effective and simple multi-attribute decision-making approach used in several applications like solar farms site selection, computer networks and process parameters selection in machining/manufacturing industries. According to TOPSIS technique, all the experimental response is segregated into beneficial or non-beneficial characteristics. Further beneficial characteristics are higher the better, and the non-beneficial characteristics are lower the better attributes. In the TOPSIS method the following steps are used to find out the multi-objective decision-making approach (Muniappan and Rajalingam, 2018).

Step I: TOPSIS decision-making formulation

Initially, the decision matrix should be created by using all the collected experimental data. The decision matrix contains y attributes and x alternative solution. In the present investigation, the output responses are attributes (y) and test trials are an alternative solution (x). The TOPSIS design matrix $D(T_{ij})_{x*y}$ is shown below

$$D(T_{ij})_{(x*y)} = \begin{bmatrix} T_{11} & T_{12} & T_{13} & \cdots & \cdots & T_{Ij} \\ T_{21} & T_{22} & T_{23} & \cdots & \cdots & T_{2j} \\ \vdots & \vdots & \vdots & \vdots & \vdots & \vdots \\ T_{i1} & T_{i2} & T_{i3} & \cdots & \cdots & T_{ij} \end{bmatrix} \quad (3)$$

WhereT_{ij} is the measure of the j^{th} attribute to the i^{th} alternative. i=1,2,3,………,x and j=1,2,3,…….,y.

Step II: Normalization of TOPSIS design matrix

The normalization of TOSIS design matrix (n_{ij}) was carried out using Eqn. (4)

$$n_{ij} = \frac{T_{ij}}{\sqrt{\sum_{i=1}^{x} {T_{ij}}^2}} \quad (4)$$

where n_{ij} is normalized value of design matrix for i=1,2,3,………..,x; j=1,2,3,………y.

Step III: Determination of weighted normalized matrix

The weights of each attribute are allocated and the sum of the weights of all attributes should be equal to 1. The weighted normalized matrix (ξ_{ij}) is calculated through the following equation

$$\xi_{ij} = w_j n_{ij} \quad (5)$$

Where$\sum_{j=1}^{y} w_j = 1$

Step IV: Identification of positive ideal solution and negative ideal solution

The positive ideal solution (ξ^+) and negative ideal solution (ξ^-) are achieved through the following equations

$\xi^{+} = (\xi_1^{+}, \xi_2^{+}, \ldots\ldots\ldots, \xi_y^{+}) = \{(\max \xi_{ij} / j \in J_1), (\min \xi_{ij} / j \in J_2, i=1,2,3,\ldots\ldots\ldots,y)$ (6)

$\xi^{-} = (\xi_1^{-}, \xi_2^{-}, \ldots\ldots\ldots, \xi_y^{-}) = \{(\min \xi_{ij} / j \in J_1), (\max \xi_{ij} / j \in J_2, i=1,2,3,\ldots\ldots\ldots,y)$ (7)

Where J_1→Set of beneficial attribute and J_2→Set of non-beneficial attribute

Step V: Calculation of separation measures

The positive separation measures (S_i^{+}) and negative separation measures (S_i^{-}) of each alternative is achieved by following equations

$$S_i^{+} = \sqrt{\sum_{j=1}^{y} (\xi_{ij} - \xi^{+})^2} \quad (8)$$

$$S_i^{-} = \sqrt{\sum_{j=1}^{y} (\xi_{ij} - \xi^{-})^2} \quad (9)$$

Step VI: Assessment of relative closeness coefficient

The estimation of relative closeness coefficient of each alternative is estimated through the following equation

$$\text{RCC} = \frac{S_i^{-}}{S_i^{+} + S_i^{-}} \quad (10)$$

Where i=1,2,3,………x.

Step VII: Ranking of alternatives

According to the performance value of relative closeness, the coefficient of each alternative is arranged and ranked in the descending order. The most suitable one (highest value) is ranked in position one and the least value is ranked in the last position.

2.4 Grey Relational Analysis method

The GRA technique is established by Deng in 1982. GRA methodology is employed to analyze the uncertainties in the system and the correlation between the systems etc. It is a mathematical oriented theory derived from the concept of the grey set. It is one of the best methods to solve uncertainty problems with incomplete information and discrete data (Rajeswari and Amirthagadeswaran, 2017). Owing to its simplicity and ability to evaluate the response within the required time, the GRA tool is mostly used in various engineering applications. GRA is a multi-response optimization method that converts the single-objective problem into a single response optimization problem. In GRA technique all the output responses are normalized between 0 and 1 for easy interpretation and data analysis purpose. These normalized output response values are used to calculate Grey relational coefficient (GRC) of every output data. The various quality characteristics of the optimization problem are normalized from 0 to 1 to generate GRC. The GRC was assessed according to the normalized experimental data. The GRC shows the correlation between the desired/ideal and actual normalized experimental results (Rajeswari and Amirthagadeswaran, 2017). Next to it, overall Grey relational grade (GRG) was obtained through averaging the GRC values respect of each experimental trial. The overall performance of an experimental trial based on GRG values. The higher the value of GRG attributes to the optimum solution of the experimental trial. The following steps were adopted in GRA

Step 1: All the experimental output responses are normalized by the following equation,

Based on the required conditions, normalization for higher-the-better

$$x_i\,(k) = \frac{g_i(k) - \min g_i(k)}{\max g_i(k) - \min g_i(k)} \tag{11}$$

Normalization for lower-the-better

$$x_i(k) = \frac{\max g_i(k) - \; g_i(k)}{\max g_i(k) - \min g_i(k)} \tag{12}$$

Where $x_i\,(k)$ is normalised value for attained experimental output response; $\min g_i(k)$ is the minimum value of $g_i(k)$ for kth response; $\max g_i(k)$ is maximum value of $g_i(k)$ for kth response; ‘i’ is the experimental number and ‘k’ is the comparability sequence.

Step 2: GRC shows the relationship between the desired and actual normalized experimental result. The GRC is computed as follows

$$\varphi_i(k) = \frac{\Delta_{min} + \; \varphi\Delta_{max}}{\Delta_{oi}(k) + \; \varphi\Delta_{max}} \tag{13}$$

Where $\Delta_{oi}(k)$ is deviation sequence,$i.e.\Delta_{oi}(k) = \; |g_i(k) - x_i(k)|$, φ is distinctive coefficient and this value lies between 0 and 1 (Normally taken as $\varphi = 0.5$) (Rajeswari and Amirthagadeswaran 2017). $\varphi_i(k)$ is a grey relational coefficient. Δ_{min} (minimum deviation sequence) is the smallest value of $\Delta_{oi}(k)$ and Δ_{max} (maximum deviation sequence) the largest value of $\Delta_{oi}(k)$.

Step 3: The average value of GRC is taken as a grey relational grade. The GRG computed as follows

$$\vartheta_i = \frac{1}{n}\sum_{i=1}^{n}\varphi_i(k) \quad (14)$$

Where ϑ_i GRG of ith trial and n is a number of trials. $\varphi_i(k)$ is a grey relational coefficient.

2.5 Thermogravimetric analysis

Thermogravimetric analysis (TGA) provides the thermal activation range of biomass (Park and Yoon 2012). The primary objective of TGA analysis is to find the degradation temperature of the given sample (Bordoloi et al., 2016). The decomposition of lignin causes sudden weight loss in the sample which can be interpreted by the steep curve in the TGA graph. The temperature at which the maximum decomposition obtained is called as ultimate decomposition temperature. The feedstock decomposition takes place in four different regions, first decomposition (T<150ºC) region is accredited to weight loss through removal of moisture content present in the biomass. The second region (200ºC<T<400ºC) is attributed to the removal of volatile matter present in the sample. The third one also called as active pyrolysis region (400ºC<T<600ºC) formed by the decomposition of organic compounds like cellulose, hemicellulose and lignin. Figure 2 shows the TGA curve of AM biomass sample. In this active pyrolysis region, cellulose, hemicellulose and lignin were decomposed in the temperature ranges of 500ºC to 600ºC. The chemical bonds present in the biomass are broken due to an elevated temperature due to which the larger molecules were converted into smaller molecular organic vapours during pyrolysis. For the AM biomass material on set, end set and the ultimate temperature are obtained from the TGA graph as 500ºC, 550ºC and 600ºC respectively.

Figure 3 shows the onset, end set temperatures, where the sudden rate of decomposition starts and end with respect to supply temperature. For AM biomass sample on set, end set and ultimate decomposition temperatures are found to be 500˚C (set), 550˚C (ultimate) and 600˚C (end) respectively. Based on the result of TGA, the maximum temperature of the pyrolytic reactor was limited to 600˚C because above which there is no decomposition observed in AM biomass sample. In the end of the decomposition region (T>600ºC), no mass loss occurs.

273 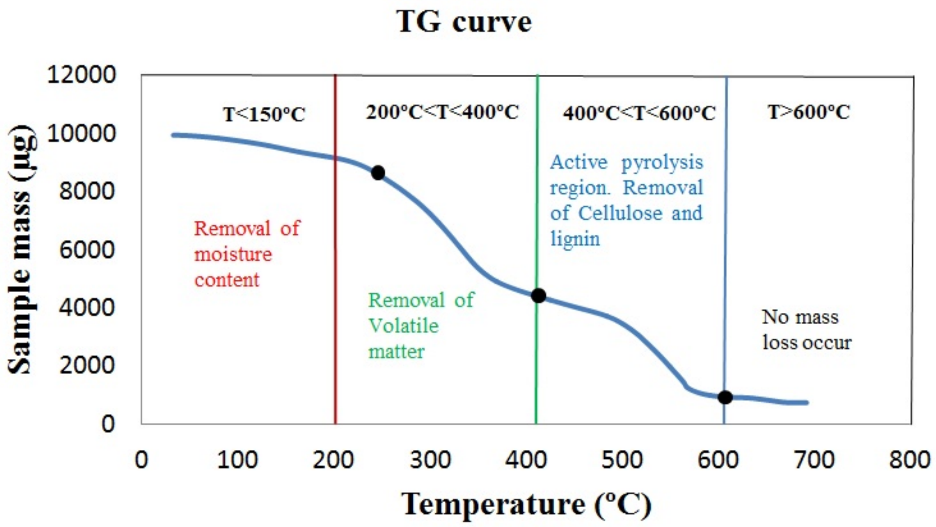

274 **Fig.2** Thermo Gravimetric analysis curve

275 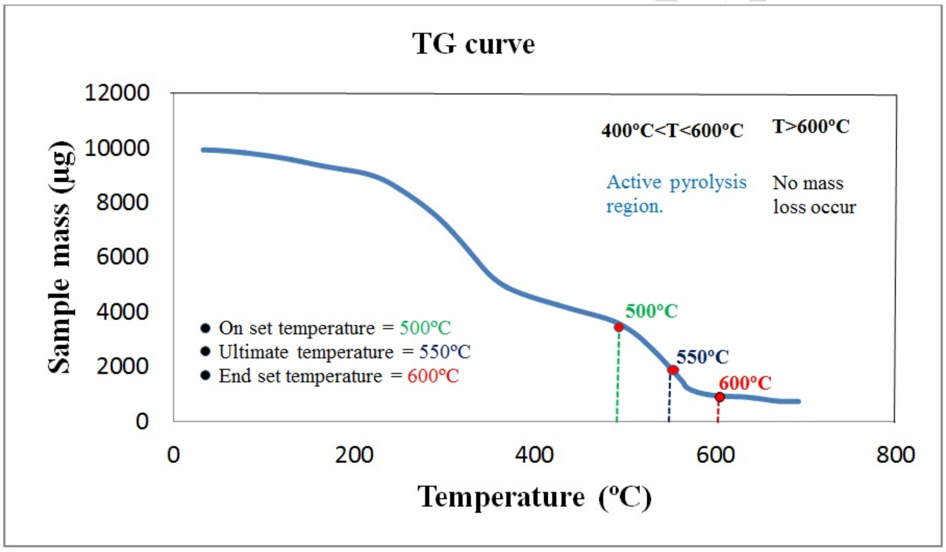

276 **Fig.3** Set Temperatures in Thermo Gravimetric analysis curve

277

278 ## 2.6 Pyrolysis experimental method

279 Figure 4 depicts the schematic diagram of a pyrolysis experimental setup. The
280 pyrolysis reactor made up of stainless steel 310 materials, in order to withstand temperature
281 upto 1000°C with inner diameter 20 mm equipped with top feeding facilities. The reactor
282 heating rate can be varied from the range of 5°C/min to 50°C/min. The fixed bed type reactor
283 is well insulated and coupled with K-type thermocouple to measure the pyrolysis
284 temperature. The reactor contains a two kilogram feed capacity with 240 V and 9.5 A
285 electrical heater for heating purpose and the reactor temperature was controlled through the
286 proportional integral derivative controller.

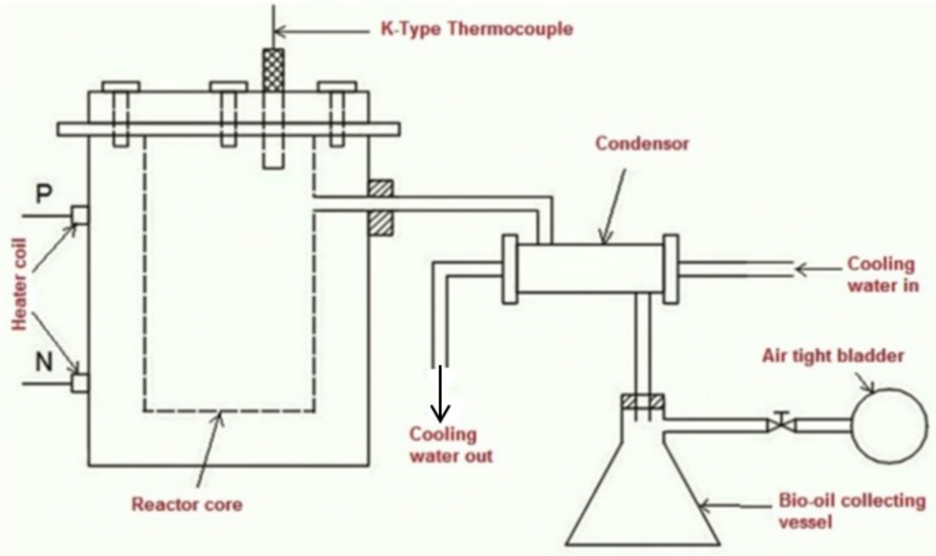

Fig.4 Schematic diagram of pyrolysisreactor

The collected AM de-oiled seed cake was crushed and sieved into different sizesby sieves shaker of 0.6 mm, 1.6 mm and 2.4 mm. Mean size of feedstock particles is classified based on particle diameter. The performance of pyrolysis experiments mainly depends upon the pyrolysis temperature, heating rate and feed stock particle size ((Halim and Swithenbank, 2016).

The yield of pyrolysis products mainly depends on the biomass properties and processing conditions (Palash et al., 2013). Pyrolysis reactor was initially cleaned properly and ensured that there is no trace of char generated by previous runs. 2 kg of sieved AM biomass is filled into the pyrolysis reactor and sealed with a gasket, to ensure that the pyrolysis reaction is carried out in absence of oxygen. The pyrolysis reactor temperature was controlled by the proportional integral derivative controller and once the thermochemical conversion process was initiated, gases were evolved and passed through the water tube condenser. The condensed pyrolytic oil was collected, whereas left out non-condensed gas was also collected in the gas bladder for gas chromatography analysis. In the end, bio-char was collected after cooling of pyrolysis reactor in atmospheric air. Every pyrolysis process was repeated at least three times to achieve reliability in the test results. Then, the mean value of the result was taken for further analysis. L_{27} (3^3) orthogonal array was used in this study and Table 3 shows the pyrolysis experimentalvalues of the input parameters with corresponding output responses.

Table 3 L_{27} orthogonal array with output response

Trial No.	Pyrolysis process parameters PT (°C)	HR (°C/min)	PS (mm)	Output response Bio-oil (wt%)	Bio-char (wt%)	Bio-gas (wt%)
1	550	10	0.6	32.92	23.44	43.64
2	550	10	1.6	36.23	23.79	39.98
3	550	10	2.4	34.50	32.15	33.35
4	550	20	0.6	35.30	34.00	30.70
5	550	20	1.6	37.93	29.91	32.16
6	550	20	2.4	36.00	35.50	28.50
7	550	30	0.6	35.50	44.10	20.40
8	550	30	1.6	37.27	33.48	29.25
9	550	30	2.4	38.75	30.85	30.40
10	600	10	0.6	42.75	30.30	26.95
11	600	10	1.6	41.39	25.58	33.03
12	600	10	2.4	40.91	37.14	21.95
13	600	20	0.6	40.51	34.73	24.76
14	600	20	1.6	40.25	29.85	29.90
15	600	20	2.4	39.89	39.10	21.01
16	600	30	0.6	38.50	42.12	19.38
17	600	30	1.6	37.21	34.30	28.49
18	600	30	2.4	36.40	33.04	30.56
19	650	10	0.6	19.45	25.55	55.00
20	650	10	1.6	26.24	21.78	51.98
21	650	10	2.4	27.00	45.50	27.50
22	650	20	0.6	16.78	22.54	60.68
23	650	20	1.6	16.15	24.25	59.60
24	650	20	2.4	26.40	42.75	30.85
25	650	30	0.6	21.12	37.25	41.63
26	650	30	1.6	19.13	21.35	59.52
27	650	30	2.4	25.75	44.25	30.00

2.7 Compression Ignitionengine test method

A single cylinder Kirloskar Co. Ltd made research engine has been used for the current experimental investigation and technical specification of the engine is given in Table 4. The CI engine coupled with AVL MDS (Modular diagnostic system) 250 gas analyser (AVL Co. Ltd, Austria) is used to analyse the emission during the engine operations. Figures 5a and 5b show the CI engine and AVL MDS 250 gas analyser. The test engine rig is incorporated with eddy current dynamometer for the purpose of providing the load to the engine during the engine operation. Based on Indian bio-fuel policy, up to 20% of biofuel can be blend with fossil fuel (Sakthivel et al., 2018). So the present work is carried out with 80%

diesel+20% AM pyrolysis oil blend (AM20) as the engine fuel and emission characteristics were analysed. The emission results were compared with standard neat diesel for further analysis. The engine was operated at different loads such as 3 kg (25%), 6 kg (50%), 9 kg (75%) and 12 kg (100%) under the steady-state conditions at 1500 rev/min and 17.5:1 standard compression ratio. The Fluke-thermal images were captured for above engine speed, CR and full engine load conditions.

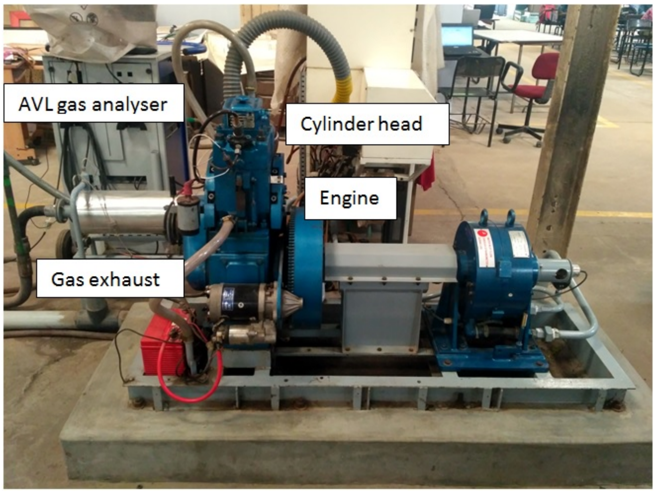

Fig. 5a Compression ignition engine

Fig.5b AVL 250 modular diagnostic system

Initially, the engine was started with diesel, and it was warmed up to 15 min at no load condition. After the engine stabilization, the experiments were conducted with blended fuels in triplicate to ensure reliability.

Table 4 Compression ignition test engine description

Description	
Manufacturer name	Kirloskar Co. Ltd
Number of cylinders	1
Number of strokes	4
Cylinder diameter	87.5 mm
Stroke length	110 mm
Connecting rod length	234 mm
Orifice diameter	20 mm
Dynamometer arm length	185
Power	3.5 kw
Speed	1500 rev/min
CR range	12:1 to 18:1

Injection point variation	0° to 25° bTDC

2.8 Fluke-Thermal imager

In this investigation, FLUKE-Thermal imager Ti400 was used to analyse exhaust gas heat during engine operation. The thermal imaging works on the principal that the Infrared (IR) energy emitted by the hot surface is converted into thermograph which implies the temperature profile of the target object (Ramesh et al., 2019). Focusing the thermal imager to the hot surface, senses the infrared energy from the hot exhaust gas during the engine operation and provides the heat distribution of the tailpipe (Sakthivel et al., 2018). The thermal imager was focused on the hot surface of the exhaust gas using a spotlight at the desired spot. The thermal imager displays the hot surface temperature distributed on the exhaust port surface and the thermal images were captured manually at the required loading condition and stored in an external pen drive for further analysis.

3. Result and discussion

3.1 Elemental analysis of biomass

Table 5 Proximate and ultimate analysis of AM bio-mass

Proximate analysis*	Weight %
Fixed carbon	21.11
Volatile matter	73.69
Ash	2.19
Moisture content	3.01
Ultimate analysis*	Weight %
Carbon	46.96
Oxygen	42.87
Nitrogen	2.56
Sulphur	0.05
Hydrogen	7.56
Calorific value (MJ/kg)	20.59

*Dry basis

Table 5 illustrates the proximate and ultimate analysis results of AM biomass material. The proximate and ultimate analysis is used to analyse the feed stock quality. The high volatile matter content of AM de-oiled seed cake was the main reason for its selection as the feed stock in this study. In typical biomass, presence of high volatile matter results in better bio-oil yield since the volatile contents are decomposed into short-chain organic vapours during pyrolysis.

The minimum percentage of fixed carbon shows the potential of the biomass material for better thermal conversion. A lesser amount of moisture content in feed stock material reveals that AM de-oiled cake can be used as a solid fuel for industrial applications. The ash content in the feed is solely based on the soil quality and plantation conditions. The ultimate analysis of the biomass shows that the de-oiled cake mainly contains carbon, hydrogen, oxygen, nitrogen and sulphur content and calorific value of biomass assure that AM seed cake can be effectively used as a feedstock material in pyrolysis experimentation.

3.2 Physical and chemical properties of bio-oil

Table 6 Physical and chemical properties of AM bio-oil

Characteristics	Unit	ASTM	AM pyrolysis oil @500ºC	AM pyrolysis oil @550ºC	AM pyrolysis oil @600ºC	Diesel
Appearance	-	-	Dark brown	Dark brown	Dark brown	Yellow
Calorific value	MJ/kg	D240	40.53	41.12	41.35	45
Viscosity	cSt@40ºC	D445	7.8	7.1	6.8	2.4
Density	g/cc @30ºC	D4052	1.401	1.102	1.055	0.845
Flash point	ºC	D93	82	79	76	65
Fire point	ºC	D93	98	93	89	74
Water content	wt%	D1744	20.7	23.5	26.4	-
Cetane number	-	D613	39	42	44	51

Table 6 illustrates the physical and chemical properties of AM bio-oil obtained as per ASTM standards. The physical and chemical properties of bio-oil depict that the viscosity of the bio-oil is higher than diesel which may affect the spray pattern and injection capabilities of the engine system (Singh and Shadangi, 2011).In this regard, it becomes essential to upgrade the bio-oil through emulsification by blending with commercial diesel fuel with the help of surfactants (Span 80 and Tween 80). However, compared to diesel, the calorific value of bio-oil is low, where it can be compensated when blended with diesel. The physical and chemical properties of the upgraded AM bio-oil show the possibility of using it as a commercial fuel in diesel engines (Singh and Shadangi, 2011).

The bio-oil contains an assorted range of compounds like methyl, ester, ether, alkanes, acids, ketones which ensure that bio-oil can be effectively used as a substitute for fossil fuels. However, it can also be used as a fuel in the furnace, agricultural generators, and boilers without up gradation (Sakthivel et al., 2018) and anti-microbial agent in pharmaceutical industries (Abas et al., 2018). The third product of the pyrolysis process is biochar, which can be used as raw material for activated charcoal production. It is confirmed that the biochar can also be used as solid fuel due to its low moisture content and high calorific value (Liew et al., 2018), cosmetic industries, waste water treatment plant, organic fertilizer (Nam et al., 2018), chemical manufacturing industries (Mohammed et al., 2017b), natural mosquito destroyer and separator for heavy metals (Lam et al., 2017). The presence of flammable components like CH_4 (Methane), H_2 (Hydrogen) and C_2H_6 (Ethane) in evolved biogas suggests that it can be used to power the pyrolysis reactor (Meier et al., 2013) and CI engines in dual fuel mode operation as gaseous fuel (Baranitharan et al., 2018).

3.3 Technique for Order Preference by Similarity to Ideal Solution analysis

In the TOPSIS technique, primarily the experimental results are altered into a decision matrix containing experimental trials (alternatives) in rows and experimental output results (attributes) in columns. Initially, the decision matrix is normalized by Eq.(4). Subsequently, relative weights are to be allocated to each attribute. In this regard the entire output responses like bio-oil yield, bio-char yield and biogas yield were given equivalent significance; hence relative weighted of 1/3 is allotted to each output result. Using Eq.(5) weighted normalized values are calculated and tabulated. Using Eqs. (6) and (7) positive ideal solutions and negative ideal solutions are evaluated from the normalized matrix. Among the entire output responses, the positive ideal solution has maximum values, which are ξ_{PT}^{+}=0.0816127, ξ_{HR}^{+} =0.087446, ξ_{PS}^{+}=0.105495 and negative the ideal solution has minimum value of weighted normalized values, that are ξ_{PT}^{-}=0.0308315, ξ_{HR}^{-}=0.041032, ξ_{PS}^{-}=0.033693. The separation measures of positive ideal solutions and negative ideal solutions are computed by Eqs.(8) and (9). Subsequently using these separation measures values, closeness coefficient of every alternative is reckoned by using Eq.(10). Table 7 represents the normalized values, weighted normalized values, separation measures values and closeness coefficient values of entire alternatives.

Table 7 Technique for order preference by similarity to the ideal solution analysis result

Trial No.	Normalization			Weighted normalization			Separation		CC
	Bio-oil	Biochar	Biogas	Bio-oil	Biochar	Biogas	S^-	S^+	
1	0.1885	0.1351	0.2276	0.062	0.0450	0.0759	0.046	0.326	0.8756543
2	0.2075	0.1372	0.2085	0.069	0.0457	0.0695	0.038	0.339	0.8988317
3	0.1976	0.1854	0.1739	0.065	0.0618	0.0580	0.035	0.333	0.9035738
4	0.2022	0.1960	0.1601	0.067	0.0653	0.0534	0.034	0.340	0.9082067
5	0.2172	0.1725	0.1677	0.072	0.0575	0.0559	0.029	0.347	0.9226872

6	0.2062	0.2047	0.1486	0.068	0.0682	0.0495	0.034	0.345	0.9104124
7	0.2033	0.2543	0.1064	0.067	0.0848	0.0355	0.045	0.362	0.8876706
8	0.2135	0.1930	0.1526	0.071	0.0643	0.0509	0.030	0.348	0.9188598
9	0.2219	0.1779	0.1586	0.074	0.0593	0.0529	0.027	0.352	0.9274789
10*	**0.2448**	**0.1747**	**0.1406**	**0.081**	**0.0582**	**0.0469**	**0.021**	**0.369**	**0.9446041**
11	0.2370	0.1475	0.1723	0.079	0.0492	0.0574	0.025	0.360	0.9346365
12	0.2343	0.2141	0.1145	0.078	0.0714	0.0382	0.030	0.371	0.9231686
13	0.2320	0.2002	0.1291	0.077	0.0667	0.0430	0.027	0.365	0.9294983
14	0.2305	0.1721	0.1559	0.076	0.0574	0.0520	0.025	0.358	0.9347756
15	0.2285	0.2254	0.1096	0.076	0.0751	0.0365	0.034	0.370	0.9144003
16	0.2205	0.2429	0.1011	0.073	0.0810	0.0337	0.040	0.370	0.9010401
17	0.2131	0.1978	0.1486	0.071	0.0659	0.0495	0.031	0.349	0.9177003
18	0.2085	0.1905	0.1594	0.069	0.0635	0.0531	0.032	0.343	0.9146600
19	0.1114	0.1473	0.2869	0.037	0.0491	0.0956	0.076	0.276	0.7827157
20	0.1503	0.1256	0.2711	0.050	0.0419	0.0904	0.064	0.305	0.8250637
21	0.1546	0.2623	0.1434	0.051	0.0874	0.0478	0.057	0.327	0.8515141
22	0.0961	0.1300	0.3165	0.032	0.0433	0.1055	0.087	0.287	0.7668190
23	0.0925	0.1398	0.3109	0.030	0.0466	0.1036	0.086	0.278	0.7627217
24	0.1512	0.2465	0.1609	0.050	0.0822	0.0536	0.055	0.315	0.8505408
25	0.1210	0.2148	0.2171	0.040	0.0716	0.0724	0.064	0.270	0.8077158
26	0.1096	0.1231	0.3104	0.036	0.0410	0.1035	0.083	0.293	0.7795702
27	0.1475	0.2551	0.1565	0.049	0.0850	0.0522	0.057	0.316	0.8458546

*Optimal condition

The alternative solution having the highest closeness coefficient (CC) value is selected as an optimum solution. In this investigation, experimental trial 10 has a maximum closeness coefficient value of 0.944604123. Among the entire experiments, the alternative trial 10 is the optimal solution and the next level of optimum solutions are experimental trial 14 and 11 respectively. The mean closeness coefficient (MCC) of every parameter at all level is computed and tabulated in Table 8. Effect of pyrolysis process parameter on MCC is depicted in Fig.6. By means of the chart, optimal process parameter for AM pyrolysis bio-oil yield is recognized as PT2HT1PS1, which are pyrolysis temperature of 600ºC, a heating rate of 10ºC/min and feedstock particle size is 0.6 mm.

Table 8 Mean closeness coefficient

	PT	HR	PS
Level I	0.905930644	**0.901293098***	**0.884598051***
Level II	**0.914881119***	0.887801476	0.880754685
Level III	0.879273190	0.827242903	0.878635601

PT- Pyrolysis temperature; HR- Heating rate; PS- Particle size

*Optimal solution

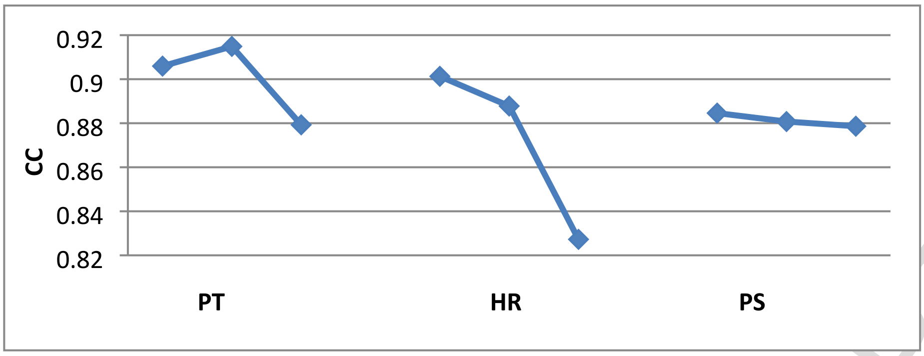

Fig.6 Effect of pyrolysis control factors on Mean closeness coefficient

3.4 Grey Relational Analysis

The main objective of the investigation is to obtain the maximum bio-oil yield from the AM de-oiled seed cake pyrolysis process. The output responses of the pyrolysis experiment were normalized for larger the better using Eq.(11) and smaller the better using Eq.(12). Table 9 illustrate the normalized value of output responses, GRC and GRG using Eqs. (11), (12), (13) and (14). For calculating the grey relational coefficient, the distinctive coefficient (φ)value is taken as 0.5 (Rajeswari and Amirthagadeswaran, 2017). In the grey relational analysis, the experimental trial having GRG near to one is selected as the optimum solution. The experimental trial number 10 have a chief grey relational grade of 0.753589 among 27 experiments, this spectacles that trial 10 affords better bio-oil yield. The pyrolysis temperature of 600ºC, heating rate of 10ºC/min and AM particle size of 0.6 mm provides the desired result among the selected input condition.

A Mean Grey relational grade (MGRG) table should be calculated by including all the parameters and their levels, in order to find out the optimal process parameters that give maximum bio-oil, bio-char and bio-gas yields. Table 10 depicts the mean grey relational grade of all parameters at each level. Considering each parameter, the level having the highest MGRG is selected as the optimal solution. From the MGRG table, the optimum process parameters are found to be pyrolysis temperature of 600ºC, a heating rate of 10ºC/min and AM particle size of 0.6 mm. Figure 7 represents the effect of pyrolysis process parameters on GRG. The result reveals that intermediate pyrolysis temperature with the lowest heating rate at small size AM particles results in maximum AM pyrolysis bio-oil yield.

Table 9 Grey relational analysis result

Trail No.	Normalized values			GRC			GRG
	Bio-oil	Bio-char	Biogas	Bio-oil	Bio-char	Biogas	
1	0.9304226	0.8262655	0.91970789	0.731585	0.876573	0.288816	0.632324
2	0.9559346	0.8301478	0.89837256	0.830005	0.856985	0.365560	0.684183
3	0.9429058	0.9090293	0.85420836	0.779742	0.458990	0.524422	0.587718
4	0.9490100	0.9236842	0.83404209	0.803291	0.385050	0.596961	0.595101
5	0.9681451	0.8901123	0.84535847	0.877110	0.554435	0.556256	0.662600
6	0.9542388	0.9349926	0.81593069	0.823463	0.327993	0.662109	0.604522
7	0.9505145	0.9918138	0.73448893	0.809095	0.041303	0.955060	0.601819
8	0.9634708	0.9196471	0.82225750	0.859078	0.405418	0.639351	0.634616
9	0.9738405	0.8982177	0.83165024	0.899082	0.513540	0.605565	0.672729
10	**1**	**0.8935057**	**0.80231016**	**1**	**0.761109**	**0.532869**	**0.753589***
11	0.9913910	0.8491501	0.85185999	0.966788	0.537314	0.711103	0.749472
12	0.9882849	0.9468221	0.75232599	0.954805	0.268308	0.890899	0.704671
13	0.9856684	0.9292486	0.78166680	0.944712	0.356974	0.785359	0.695682
14	0.9839539	0.8895864	0.82761087	0.938097	0.557089	0.620095	0.705094
15	0.9815615	0.9602930	0.74166534	0.928868	0.200341	0.929246	0.686152
16	0.9721170	0.9797812	0.72199551	0.892433	0.102014	1	0.664816
17	0.9630418	0.9259853	0.81584522	0.857423	0.373440	0.662417	0.631093
18	0.9571812	0.9161819	0.83292881	0.834814	0.422902	0.600966	0.619561
19	0.7902944	0.8488427	0.97605963	0.190998	0.762660	0.086115	0.346591
20	0.8700303	0.8070257	0.96230431	0.498603	0.973647	0.135594	0.535948
21	0.8776332	1	0.80723090	0.527934	0	0.693403	0.407112
22	0.7509748	0.8160100	1	0.039311	0.928317	0	0.322545
23	0.7407847	0.8351642	0.99562362	0	0.831675	0.015742	0.282472
24	0.8716491	0.9836700	0.83522926	0.504848	0.082392	0.592691	0.393310
25	0.8122292	0.9475968	0.90822288	0.275618	0.264399	0.330128	0.290049
26	0.7858769	0.8018026	0.99529647	0.173956	1	0.016919	0.396958
27	0.8650107	0.9927032	0.82842412	0.479239	0.036816	0.617169	0.377741

*Optimal solution

Table 10 Mean grey relational grade

	PT	HR	PS
Level 1	0.630624	**0.62740***	**0.578551***
Level 2	**0.660319***	0.59057	0.571566
Level 3	0.564388	0.564388	0.564388

PT- Pyrolysis temperature; HR- Heating rate; PS- Particle size

*Optimal condition

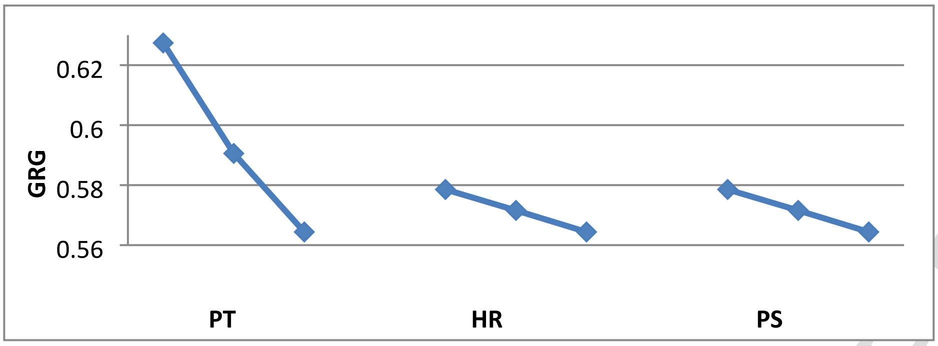

Fig.7 Effect of pyrolysis process parameter on Grey Relational Grade

3.5 Comparison of Technique for order preference by similarity to ideal solution and Grey relational analysis output responses

The optimum output responses obtained from TOPSIS and GRA techniques are compared. It can be observed that both the optimization tools give a similar combination of pyrolysis process parameters PT2HR1PS1as optimum solution. The output result confirms that TOPSIS tool executes efficiently like GRA tool and can be employed for multi-objective problem optimization.

3.6 Compression Ignition engine emission characteristics

Diesel engines are the foremost important engineering invention in the commercial engineering sectors (Ferguson and Kirkpatrick, 2015). At the same time, diesel engines emit the harmful gases into the atmosphere. Bio-fuel emits a lower amount of pollutants as compared to fossil fuels, owing to its rich oxygen content (Emberger et al., 2015). With the help of AVL gas analyser, exhaust gases like CO (Carbon monoxide), HC (Hydro carbons), NOx and CO_2 emissions are analysed during engine operation. Figures 8a-d represents the CO, HC, CO_2 and NOx emissions compared with neat diesel fuel.

Incomplete combustion and insufficient air-fuel mixing ratio generate CO emission at engine exhaust (Atmanlı et al., 2014). Figure 8a represents the comparison between CO emission of AM bio-oil and diesel fuel. According to the figure, AM bio-oil blends emit a higher amount of CO as compared with diesel. The high viscosity and density (1.401, 1.102 and 1.055 g/cc @30ºC) of the AM fuel blends compared with neat diesel (0.845 g/cc @30ºC) leads to the poor atomization and incomplete combustion during combustion (Hellier et al., 2015). At the full load condition, diesel emits 0.17% volume of CO and AM20 blend emits 0.44% volume of CO emission.

Figure 8b illustrates the comparison between the effects of neat diesel and AM blend on HC emission with respect to load. The inadequate combustion of fuel molecules emits the HC (Wamankar et al., 2015). In general, the fuel having a high viscosity leads to poor atomization during the fuel injection, which in turn causes the HC emission. The viscosity difference between AM fuel blends (7.8, 7.1 and 6.8 cSt@40°C) with neat diesel (2.4 cSt@40°C) augments the higher amount of HC emission as compared to neat diesel since the kinematic viscosity of bio-oil does not meet the diesel fuel ASTM standards (Shameer and Ramesh, 2017a). At full load, condition dieselemits 58 ppm of HC and AM20 blend emits 99 ppm of HC. AM20 blend emits the higher value of HC compare to baseline fuel, due to high viscosity and poor injection spray characteristics (Muniappan and Rajalingam, 2018).

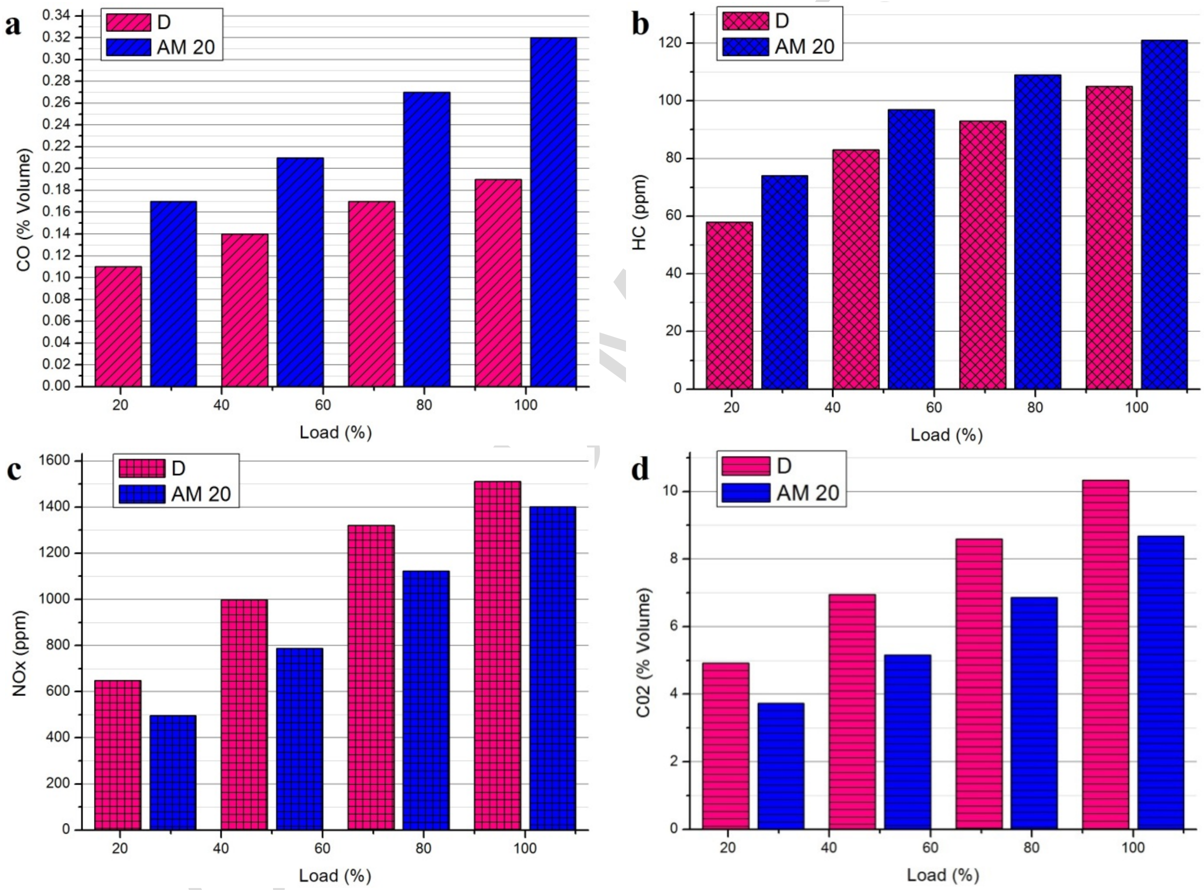

Fig.8 Compression ignition engine emission characteristics

At high temperatures around 1500ºC, nitrogen and oxygen in combustion chamber react to form the respective oxides via a sequence of chemical reactions called as Zeldovich mechanism (Paramasivam et al., 2018; Sakthivel et al., 2018). Based on the Zeldovich mechanism, maximum thermal NOx emission is caused by higher temperature in the combustion chamber during the engine operation (Baranitharan et al., 2018)). Figure 8c spectacles the NOx emissions of diesel and AM20 fuel blend with respect to load. At peak load condition D emits 1511 ppm of NOx and AM20 blend emits 1401 ppm of NOx. It can be due to the fact that, increasing load obviously increases the combustion chamber temperature and also the quenching effect of water content present in the pyrolysis oil reduces the flame temperature, thereby emitting less magnitude of NOx (Corsini et al., 2015).

Figure 8d represents the CO_2 emission of both AM fuel blends and neat diesel. The complete combustion of fuel in the combustion chamber is straight away indicated by CO_2 emission (Sakthivel et al., 2018). Muniappan and Rajalingam (2018) optimized the performance and emission behaviours of a diesel engine fuelled with bael oil (25%) + diesel (65%) + Di-ethyl ether (10%) fuel blend using TOPSIS and found that brake thermal efficiency increased 28.6%, CO reduced 0.025% and HC reduced 12.5 ppm. At low load condition, the CO_2 emission for diesel and AM fuel blends is lower. This reduction is caused by the lower combustion temperature and the inefficient burning of fuel (Muniappan and Rajalingam, 2018). But, CO_2 emission consequently increased with increase in load for both diesel and fuel blend ratio, due to increasing combustion temperature. Throughout the engine operation, the CO_2 emission level was noted to increase with respect to load. As compare to AM fuel blends, diesel emits a higher amount of CO_2 at all load condition. It is depicted that, fuel blends were involved in better combustion as compared to diesel (Shameer and Ramesh, 2017a). At full load, condition diesel emits 10.33% of CO_2 and AM20 blend emits 8.68% of CO_2.

3.7 Fluke-Thermal images validation

Figure 9a illustrates the location of the thermal image for the measurement of exhaust gas temperature (heat). Figures9b-9d shows the exhaust gas temperature of AM bio-oil derived from various pyrolysis temperatures are 600ºC, 550ºC and 500ºC respectively. In Fig.9e, the exhaust gas temperature of diesel fuel has been portrayed. Once the combustion process takes place in the in-cylinder chamber, the combustion chamber temperature raises. The heat inside the combustion chamber flows via the cylinder and exhaust port. The distributed heat on the exhaust port was sensed by using thermal imager. The IR thermal images depict that the combustion chamber heat is distributed via cylinder head and exhaust port emission (Shameer and Ramesh, 2017a). In engine operation, when combustion chamber temperature increases at peak load condition, apparently engine components heat also highly increases (Shameer and Ramesh, 2017b). During the engine operation, a higher value of combustion chamber temperature leads to a higher amount of NOx emission (Hellier et al., 2015).

The location of the temperatures is mainly focused to exhaust port of the test engine setup. In thermal images, boring tool temperature selected, according to the representation "MAX", "MIN", and average values. "MAX" and "MIN" indicates the maximum and minimum temperatures of the boring tool surface during machining operation and center value is indicated the average tool (actual temperature) temperature value.

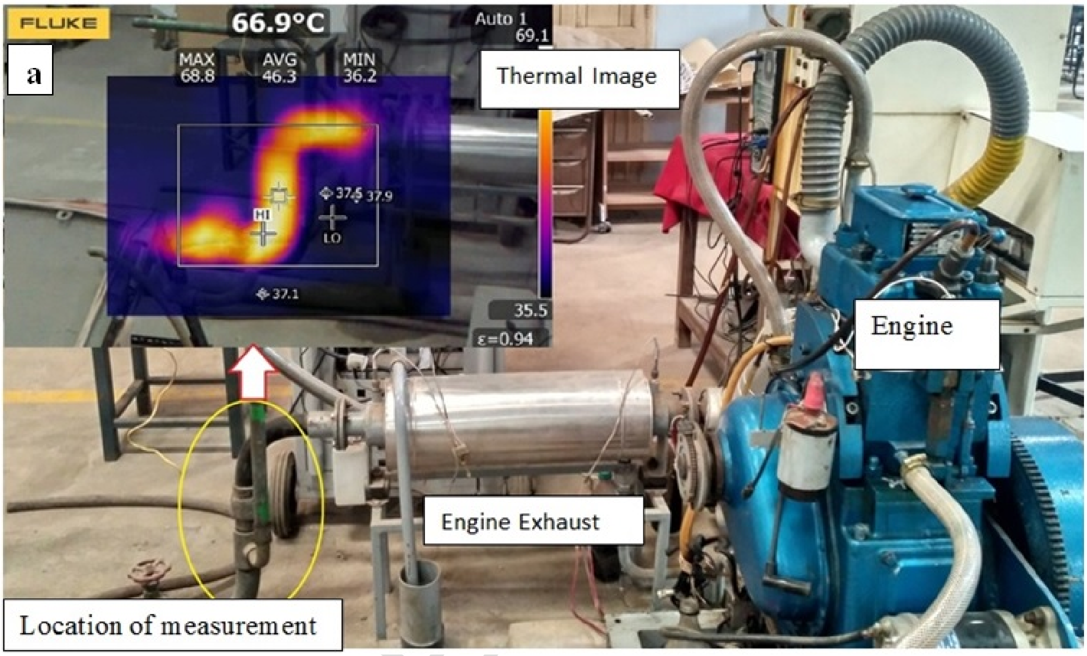

Fig.9a Location of measurement

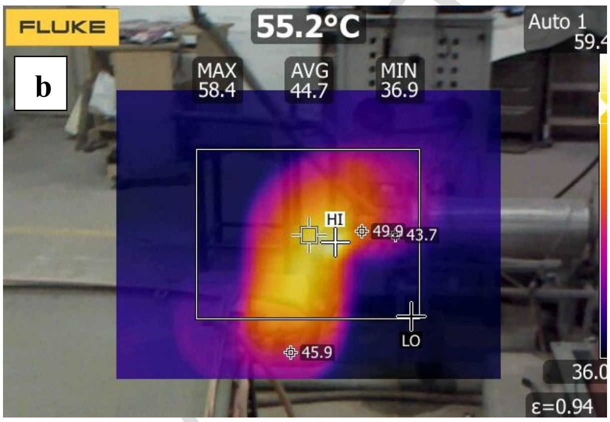

Fig.9b Exhaust gas temperature of AM pyrolysis oil obtained from 600 °C

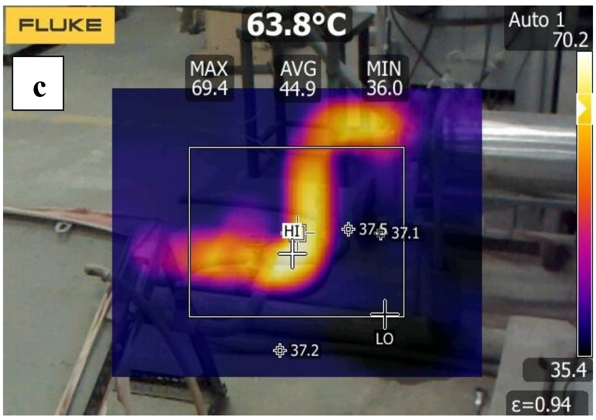

Fig.9C Exhaust gas temperature of AM pyrolysis oil obtained from 600 °C

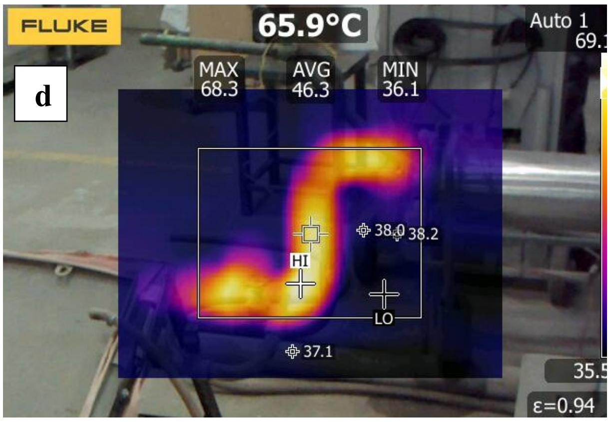

Fig.9d Exhaust gas temperature of AM pyrolysis oil obtained from 600 °C

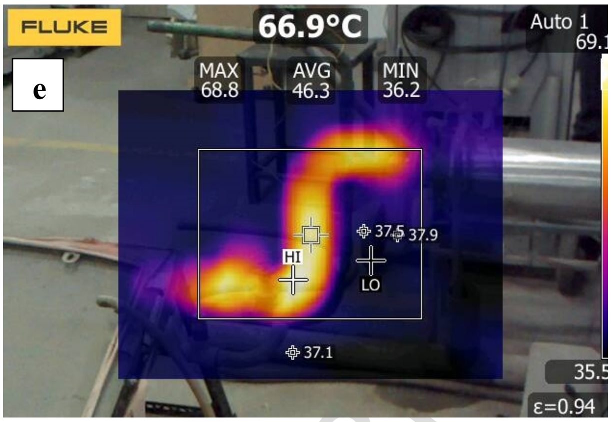

Fig.9e Exhaust gas temperature of diesel

A Non-contacting measuring technique gives accurate values than contact measuring methods. The NOx emission value is greatly temperature dependent. The quenching effect of moisture present in the pyrolysis oil (Moisture content= 20.7% @500ºC, 23.5% @550ºC and 26.4% @600ºC) reduces the flame temperature (Corsini et al., 2015) thereby decreases the amount of NOx as compared to diesel. According to the thermal images result, the low exhaust gas temperature was recorded for AM bio-oil obtained at PT =600ºC, HR=10ºC/min, PS=0.6 mm. It conforms that AM pyrolysis oil emits lower emission of NOx compare to plain diesel during engine operation. From the thermal imaging, it can be seen that augmented gas temperature of diesel operation resulted in augmentation of NOx, whereas the reduction in NOx was validated through reduced gas temperature as exhaust during AM bio-oil operation (Garcia-Gonzalez et al., 2016).

3.8 Practical implications and Future work

Stability of bio-oil is one of the inevitable characteristics, which influences the commercialization of the fuel market. In general, bio-oil possesses poor stability characteristics due to the presence of reactive organic compounds. This, in turn, affects the physical and chemical properties of bio-oil during the prolonged storage period. Thermal and oxidative degradation affect the decomposition of compounds present in the bio-oil and catalyses polymerization reaction which increases the viscosity, water content, gumming activity and solid content. In this regard, it is mandatory to investigate bio-oil storage stability. Since biochar contains an acceptable amount of carbons, it can be used as a composites reinforcement face, nanotubes manufacturing and can also be used in the material manufacturing industry as a catalyst instead of carbons.

4. Conclusion

The requirements for fuel energy and reduced exhaust emissions of CI engines can be accomplished by biofuel research. The aim of the present research work is to attain the maximum bio-oil yield, in order to fulfil the energy requirements. The present AM pyrolysis work considers pyrolysis temperature, heating rate and particle size as the input criteria to obtain optimum pyrolysis condition for maximizing the bio-oil yield. At optimized pyrolysis conditions, the maximum AM bio-oil, bio-char and biogas yields were 42.75, 30.30 and 26.95 (wt%) respectively. At peak load conditions AM20 bio-fuel blend emits lower NOx of 15.97% and lesser CO_2 of 7.28% as compared with D fuel and emission characteristics are validated through a novel approach using FLUKE-thermal imager. Infrared thermography images were confirmed the same NOx emission results for both D and AM20 fuel. According to the emission results, as compared to D fuel, AM20 fuel blend emits lesser amounts of harmful emissions at the exhaust. This depicts that AM20 is suitable for engine fuel in terms of emission reduction. This investigation shows that similar results were obtained for both TOPSIS and GRA techniques and they can be used as effective tools to optimize the multi-objective problem in AM pyrolysis experimental process and attain the maximum bio-oil yield through optimized process parameters (PT=600°C, HR=10°C/min and PS=0.6 mm).

References

Abas, F.Z., Ani, F.N., Zakaria, Z.A., 2018. Microwave-assisted production of optimized pyrolysis liquid oil from oil palm fiber. Journal of cleaner production 182, 404-413.

Anupam, K., Lal, P.S., Bist, V., Sharma, A.K., Swaroop, V., 2014. Raw material selection for pulping and papermaking using TOPSIS multiple criteria decision making design. Environmental Progress & Sustainable Energy 33(3), 1034-1041.

Anupam, K., Sharma, A.K., Lal, P.S., Dutta, S., Maity, S., 2016. Preparation, characterization and optimization for upgrading Leucaena leucocephala bark to biochar fuel with high energy yielding. Energy 106, 743-756.

Atmanlı, A., Ileri, E., Yüksel, B., 2014. Experimental investigation of engine performance and exhaust emissions of a diesel engine fueled with diesel–n-butanol–vegetable oil blends. Energy Conversion and Management 81, 312-321.

Baranitharan, P., Ramesh, K., Sakthivel, R., 2018. Analytical characterization of the Aegle marmelos pyrolysis products and investigation on the suitability of bio-oil as a third generation bio-fuel for CI engine. Environmental Progress & Sustainable Energy.

Baranitharan, P., Ramesh, K., Sakthivel, R., 2019. Measurement of performance and emission distinctiveness of Aegle marmelos seed cake pyrolysis oil/diesel/TBHQ opus powered in a DI diesel engine using ANN and RSM. Measurement.

Bordoloi, N., Narzari, R., Sut, D., Saikia, R., Chutia, R.S., Kataki, R., 2016. Characterization of bio-oil and its sub-fractions from pyrolysis of Scenedesmus dimorphus. Renewable energy 98, 245-253.

Chen, G.-L., Chen, G.-B., Li, Y.-H., Wu, W.-T., 2014. A study of thermal pyrolysis for castor meal using the Taguchi method. Energy 71, 62-70.

Corsini, A., Marchegiani, A., Rispoli, F., Sciulli, F., Venturini, P., 2015. Vegetable oils as fuels in Diesel engine. Engine performance and emissions. Energy procedia 81, 942-949.

D'Alessandro, B., Bidini, G., Zampilli, M., Laranci, P., Bartocci, P., Fantozzi, F., 2016. Straight and waste vegetable oil in engines: Review and experimental measurement of emissions, fuel consumption and injector fouling on a turbocharged commercial engine. Fuel 182, 198-209.

Emberger, P., Hebecker, D., Pickel, P., Remmele, E., Thuneke, K., 2015. Ignition and combustion behaviour of vegetable oils after injection in a constant volume combustion chamber. Biomass and bioenergy 78, 48-61.

Ferguson, C.R., Kirkpatrick, A.T., 2015. Internal combustion engines: applied thermosciences. John Wiley & Sons.

Garcia-Gonzalez, J.C., Moscoso-Kingsley, W., Madhavan, V., 2016. Tool rake face temperature distribution when machining Ti6Al4V and Inconel 718. Procedia Manufacturing 5, 1369-1381.

Guo, S., Zhao, H., 2015. Optimal site selection of electric vehicle charging station by using fuzzy TOPSIS based on sustainability perspective. Applied Energy 158, 390-402.

Halim, S.A., Swithenbank, J., 2016. Characterisation of Malaysian wood pellets and rubberwood using slow pyrolysis and microwave technology. Journal of analytical and applied pyrolysis 122, 64-75.

Hellier, P., Ladommatos, N., Yusaf, T., 2015. The influence of straight vegetable oil fatty acid composition on compression ignition combustion and emissions. Fuel 143, 131-143.

Hussain, M., Peethambaran, K., Ushakumari, E., 2014. Performance Optimization of Diesel Engine with Chicken Waste Bio-diesel Blend Using Grey Rrelational Aanalysis. International Journal of Engineering Research and Development 10(11), 09-15.

Hussein, Y.S., Ali, B.M., Rasid, M.F.A., Sali, A., Mansoor, A.M., 2016. A novel cell-selection optimization handover for long-term evolution (LTE) macrocellusing fuzzy TOPSIS. Computer Communications 73, 22-33.

Katagi, K.S., Munnolli, R.S., Hosamani, K.M., 2011. Unique occurrence of unusual fatty acid in the seed oil of Aegle marmelos Corre: Screening the rich source of seed oil for bio-energy production. Applied energy 88(5), 1797-1802.

Knothe, G., Sharp, C.A., Ryan, T.W., 2006. Exhaust emissions of biodiesel, petrodiesel, neat methyl esters, and alkanes in a new technology engine. Energy & Fuels 20(1), 403-408.

Kuo, Y., Yang, T., Huang, G.-W., 2008. The use of grey relational analysis in solving multiple attribute decision-making problems. Computers & industrial engineering 55(1), 80-93.

Lam, S.S., Liew, R.K., Wong, Y.M., Yek, P.N.Y., Ma, N.L., Lee, C.L., Chase, H.A., 2017. Microwave-assisted pyrolysis with chemical activation, an innovative method to convert orange peel into activated carbon with improved properties as dye adsorbent. Journal of cleaner production 162, 1376-1387.

Liew, R.K., Chong, M.Y., Osazuwa, O.U., Nam, W.L., Phang, X.Y., Su, M.H., Cheng, C.K., Chong, C.T., Lam, S.S., 2018. Production of activated carbon as catalyst support by microwave pyrolysis of palm kernel shell: a comparative study of chemical versus physical activation. Research on Chemical Intermediates 44(6), 3849-3865.

Liu, H.-T., Cheng, H.-S., 2016. An improved grey quality function deployment approach using the grey TRIZ technique. Computers & Industrial Engineering 92, 57-71.

López, P.R., Jurado, F., Reyes, N.R., Galán, S.G., Gómez, M., 2008. Particle swarm optimization for biomass-fuelled systems with technical constraints. Engineering Applications of Artificial Intelligence 21(8), 1389-1396.

Madhu, P., Kumar, C.N., Anojkumar, L., Matheswaran, M., 2018. Selection of biomass materials for bio-oil yield: a hybrid multi-criteria decision making approach. Clean Technologies and Environmental Policy 20(6), 1377-1384.

Meier, D., Van De Beld, B., Bridgwater, A.V., Elliott, D.C., Oasmaa, A., Preto, F., 2013. State-of-the-art of fast pyrolysis in IEA bioenergy member countries. Renewable and Sustainable Energy Reviews 20, 619-641.

Merino-Pérez, J.L., Royer, R., Ayvar-Soberanis, S., Merson, E., Hodzic, A., 2015. On the temperatures developed in CFRP drilling using uncoated WC-Co tools Part I: Workpiece constituents, cutting speed and heat dissipation. Composite Structures 123, 161-168.

Mi, B., Liu, Z., Hu, W., Wei, P., Jiang, Z., Fei, B., 2016. Investigating pyrolysis and combustion characteristics of torrefied bamboo, torrefied wood and their blends. Bioresource technology 209, 50-55.

Mohammed, I.Y., Abakr, Y.A., Hui, J.N.X., Alaba, P.A., Morris, K.I., Ibrahim, M.D., 2017a. Recovery of clean energy precursors from Bambara groundnut waste via pyrolysis: Kinetics, products distribution and optimisation using response surface methodology. Journal of cleaner production 164, 1430-1445.

Mohammed, I.Y., Abakr, Y.A., Yusup, S., Kazi, F.K., 2017b. Valorization of Napier grass via intermediate pyrolysis: Optimization using response surface methodology and pyrolysis products characterization. Journal of cleaner production 142, 1848-1866.

Muniappan, K., Rajalingam, M., 2018. TOPSIS-based parametric optimization of compression ignition engine performance and emission behavior with bael oil blends for different EGR and charge inlet temperature. Environmental Science and Pollution Research 25(19), 19040-19053.

Nam, W.L., Phang, X.Y., Su, M.H., Liew, R.K., Ma, N.L., Rosli, M.H.N.B., Lam, S.S., 2018. Production of bio-fertilizer from microwave vacuum pyrolysis of palm kernel shell for cultivation of Oyster mushroom (Pleurotus ostreatus). Science of the total environment 624, 9-16.

Palash, S., Masjuki, H., Kalam, M., Masum, B., Sanjid, A., Abedin, M., 2013. State of the art of NOx mitigation technologies and their effect on the performance and emission characteristics of biodiesel-fueled Compression Ignition engines. Energy conversion and management 76, 400-420.

Paramasivam, B., Kasimani, R., Rajamohan, S., 2018. Characterization of pyrolysis bio-oil derived from intermediate pyrolysis of Aegle marmelos de-oiled cake: study on performance and emission characteristics of CI engine fueled with Aegle marmelos pyrolysis oil-blends. Environmental Science and Pollution Research 25(33), 33806-33819.

Rajeswari, B., Amirthagadeswaran, K., 2017. Experimental investigation of machinability characteristics and multi-response optimization of end milling in aluminium composites using RSM based grey relational analysis. Measurement 105, 78-86.

Ramesh, K., Baranitharan, P., Sakthivel, R., 2019. Investigation of the stability on boring tool attached with double impact dampers using Taguchi based Grey analysis and cutting tool temperature investigation through FLUKE-Thermal imager. Measurement 131, 143-155.

Sahu, P.K., Kumari, K., Pal, S., Pal, S.K., 2016. Hybrid fuzzy-grey-Taguchi based multi weld quality optimization of Al/Cu dissimilar friction stir welded joints. Advances in Manufacturing 4(3), 237-247.

Sakthivel, R., Ramesh, K., Purnachandran, R., Shameer, P.M., 2018. A review on the properties, performance and emission aspects of the third generation biodiesels. Renewable and Sustainable Energy Reviews 82, 2970-2992.

Senthilkumar, N., Deepanraj, B., Vasantharaj, K., Sivasubramanian, V., 2016. Optimization and performance analysis of process parameters during anaerobic digestion of food waste using hybrid GRA-PCA technique. Journal of Renewable and Sustainable Energy 8(6), 063107.

Shameer, P.M., Ramesh, K., 2017a. Experimental evaluation on performance, combustion behavior and influence of in-cylinder temperature on NOx emission in a DI diesel engine using thermal imager for various alternate fuel blends. Energy 118, 1334-1344.

Shameer, P.M., Ramesh, K., 2017b. Study on clean technology-assisted combustion behavior and NO x emission using thermal imager for alternate fuel blends. International journal of environmental science and technology 14(12), 2759-2768.

shen How, B., Lam, H.L., 2018. Sustainability evaluation for biomass supply chain synthesis: novel principal component analysis (PCA) aided optimisation approach. Journal of Cleaner Production 189, 941-961.

Singh, R., Shadangi, K., 2011. Liquid fuel from castor seeds by pyrolysis. Fuel 90(7), 2538-2544.

Wamankar, A.K., Satapathy, A.K., Murugan, S., 2015. Experimental investigation of the effect of compression ratio, injection timing & pressure in a DI (direct injection) diesel engine running on carbon black-water-diesel emulsion. Energy 93, 511-520.
Wang, S., Jiang, X., Wang, Q., Han, X., Ji, H., 2013. Experiment and grey relational analysis of seaweed particle combustion in a fluidized bed. Energy conversion and management 66, 115-120.

HIGHLIGHTS

- Pyrolysis oil was derived from the AM seed cake
- AM pyrolysis process parameters are optimized through TOPSIS and GRA
- Both TOPSIS and GRA techniques showed similar results
- Bio-oil was used as an alternative fuel in CI engine
- NOx emission behaviour is validated through Thermal images